Preparation and Characterization of Cellulose Nanocrystals from Paper Mulberry Fibers

Hae Min Jo,[a] Soo Hyun Lee,[a] and Ji Young Lee [b,*]

The applicability of paper mulberry fiber (PM-FB), which is bast fiber, for manufacturing cellulose nanocrystals (CNCs) with high-yield was investigated. The PM-FB and hardwood bleached kraft pulp (Hw-BKP) were hydrolyzed under different sulfuric acid concentrations, reaction times, and reaction temperatures. The dependence of the CNC yield on the hydrolysis conditions and crystallinity of the raw materials was analyzed. The functional groups of the CNCs and their zeta potentials were determined. The fiber length and width of the individual CNCs were determined by transmission electron microscopy image analysis. The PM-FB showed a higher crystallinity of 86.8% compared to that of Hw-BKP and exhibited a high CNC yield of 55% under strong hydrolysis conditions. The sulfate group was introduced into the CNCs, which increased their negative charge. The fiber width of PM-FB-based CNCs (PM-CNCs) was larger than that of Hw-BKP-based CNCs (Hw-CNCs), and the aspect ratio ranged from 29.0 to 12.2 depending on the hydrolysis conditions. The yield of PM-CNCs was higher than that of Hw-CNCs under the same hydrolysis conditions. In addition, both CNCs exhibited similar quality. Therefore, PM-FB is a promising raw material for efficient CNC manufacturing.

DOI: 10.15376/biores.18.2.4055-4070

Keywords: Bast fiber; Paper mulberry; Cellulose nanocrystal; Yield; Aspect ratio

*Contact information: a: Department of Forest Products, Gyeongsang National University, Jinju 52828, Republic of Korea; b: Department of Environmental Materials Science/IALS, Gyeongsang National University, Jinju 52828, Republic of Korea; *Corresponding author: paperyjy@gnu.ac.kr*

INTRODUCTION

The interest in eco-friendly materials increases with increased global interest in environmental conservation (Rajinipriya *et al*. 2018). Cellulose resources are one of the most naturally abundant renewable materials (Kargupta *et al*. 2021). Thus, several studies have been conducted to replace nonbiodegradable synthetic polymers with natural cellulosic materials (Thakur *et al*. 2018; Arun *et al*. 2022; Moshood *et al*. 2022; Samir *et al*. 2022). Cellulose, which is a biodegradable natural material, is a linear polymer containing β-1,4 glycosidic bonds between glucose units (Li *et al*. 2021; Seddiqi *et al*. 2021). Cellulose fiber, which is composed of cellulose chains, can be obtained from various wood and non-wood resources and is a major resource for nanocellulose manufacturing (de Souza Fonseca *et al*. 2019). Nanocellulose, which is a material composed predominantly of cellulose with nanoscale external dimensions, is considered an alternative for plastic materials because of its unique characteristics and eco-friendliness (Hu *et al*. 2020; Zinge and Kandasubramanian 2020). In particular, cellulose nanocrystals (CNCs) manufactured based on the chemical treatment of cellulose fiber is a promising

material for manufacturing eco-friendly flexible packaging materials, conductive films, and substrates because of its excellent mechanical and optical properties, *e.g.*, transparency (Grishkewich *et al.* 2017; Guo and Guo 2022). CNCs are typically fabricated from wood pulp such as hardwood bleached kraft pulp (Hw-BKP) and softwood bleached kraft pulp (Sw-BKP). Studies have reported low CNC yield (20% to 30%) from these materials using strong acid hydrolysis conditions (Lin *et al*. 2019; Kandhola *et al*. 2020). There are various methods to increase the CNC yield; however, it is essential to find a more appropriate raw material that can be converted into CNC under mild hydrolysis conditions.

Bast fiber is derived from the outer layers of plant stems, *i.e.*, from the fiber bundle in the area between the bark and phloem tissue. Bast fibers can be obtained from various types of plants, such as yellow horse, flax, as well as paper mulberry and kenaf (George and Sabapathi 2015). Bast fibers are long (length > 50 mm) and durable, with their tensile strength higher than that of wood fibers (Yu *et al.* 2019). Moreover, they have lower lignin content than woody fibers and exhibit higher crystallinity than other natural fibers (Jones *et al*. 2017). While the proportion of bast fibers to the total weight of the wood is low, these fibers are of high quality with high density and strength, resulting in a high yield of usable fibers. Thus, bast fibers can be used as good raw material for natural polymer.

To produce CNC, the commonly used method is the hydrolysis using hydrochloric acid, phosphoric acid, or sulfuric acid, and various techniques such as mechanical and enzymatic treatment can also be applied as needed (Domingues *et al*. 2014; George and Sabapathi 2015; Tang *et al*. 2022). In particular, sulfuric acid hydrolysis is an effective method for obtaining a suspension with a high colloidal stability by introducing a sulfate group into the hydroxyl group of cellulose (Dong *et al*. 2016). In this study, CNCs made of paper mulberry fiber (PM-FB), which is a bast fiber, were manufactured and compared with CNCs made of wood-based fibers to evaluate its manufacturing feasibility. The CNC suspensions were obtained using two kinds of pulps in the reaction under different hydrolysis conditions. The ionic charge properties of the manufactured CNC particles and Fourier transform infrared (FT-IR) spectroscopy analysis confirmed the introduction of sulfate group. The fiber size was measured and X-ray diffraction (XRD) analysis was conducted to compare the fiber quality. Finally, high-yield CNCs were obtained using PM-FB, and the PM-CNC characteristics were assessed to evaluate their potential as an eco-friendly raw material for nanocellulose manufacturing.

EXPERIMENTAL

Materials

PM-FB (Fig. 1A) was obtained from the Forest Biomaterials Research Center (Jinju, Republic of Korea) and was used to fabricate CNCs.

Hw-BKP (Fig. 1B) was obtained from Moorim Paper (Jinju, Republic of Korea). H_2SO_4 (98%, Daejung Chemicals & Metals Co., Ltd., Siheung, Republic of Korea) was used for acid hydrolysis, and a dialysis tube (Spectra/Por 4 12-14kD MWCO, Spectrum Labs, San Francisco, CA, USA) was used for washing the material by membrane dialysis after the completion of the reaction.

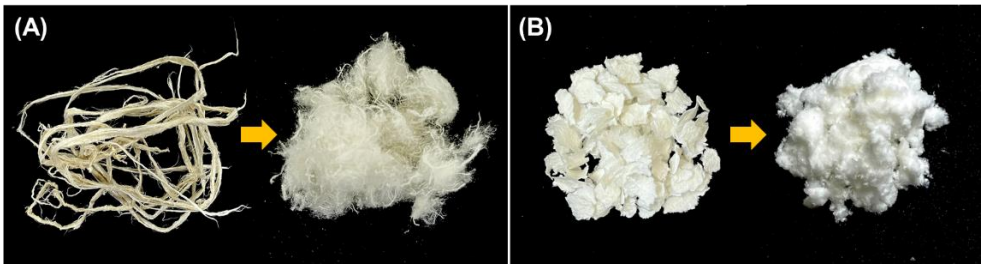

Fig. 1. Images of (A) PM-FB, and (B) Hw-BKP

Methods

CNC Preparation from different pulps

The air-dried pulp samples PM-FB and Hw-BKP were mechanically treated using a laboratory blender (SHMF-3000S, Hanil Electric, Bucheon, Republic of Korea) for 10 min and 3 min, respectively, in preparation for sulfuric acid hydrolysis. The mechanically processed samples exhibited a fluffy texture (Fig. 1), and they were stored at room temperature before the experiment. The PM-FB and Hw-BKP fibers were hydrolyzed using a diluted sulfuric acid solution (100 mL) under continuous stirring. As shown in Table 1, different hydrolyzing conditions, *i.e.*, sulfuric acid concentration, reaction time, and temperature, were assessed. When paper mulberry fibers were hydrolyzed with a 55% sulfuric acid solution for 30 minutes, fibrous residue was still present, making this hydrolysis condition unsuitable for analyzing the characteristics of CNC. This could be attributed to the considerably longer fiber length of paper mulberry fibers compared to that of woody fibers (Cong and Dong 2007; Park *et al*. 2019). After increasing the reaction time to 45 minutes, stirring between the paper mulberry fiber and sulfuric acid solution improved and hydrolysis reaction smoothly. The ratio of the fiber to the sulfuric acid solution was set at 1:20 (g/mL) under all conditions. 100 mL of cold distilled water was added to the cellulose suspension to stop the reaction. The suspension was then centrifuged 10 times at 5,000 rpm for 30 min each. The separated supernatant in each step was replaced by distilled water and mixed with the precipitate under strong agitation for 5 min. This process was repeated until the supernatant became turbid, and the colloidal suspension was collected. The collected supernatant was washed using membrane dialysis for 4 days to remove the sulfuric acid and sugars. After dialysis, the CNC suspensions (pH = 6.8 to 7.0) were dispersed for 5 min by sonication and then stored in a refrigerator at 4 °C.

Table 1. Fiber Width and Average Particle Size of NFCs

Raw Materials	Concentration of H_2SO_4 (%)	Time (min)	Temperature (°C)
PM-FB	55	30	-
	55	45	50, 60, 70
	60	30	50, 60, 70
	60	45	50, 60, 70
Hw-BKP	55	30	50, 60, 70
	55	45	50, 60, 70
	60	30	50, 60, 70
	60	45	50, 60, 70

Yield analysis of CNCs

The yields of CNC according to the type of cellulose fiber and conditions of sulfuric acid hydrolysis were investigated. The total yield was calculated based on the weight (W_1) and consistency (W_2) of the CNC suspensions. Here, CNC suspension refers to the suspension obtained after removing residue and decomposed sugars through centrifugation and membrane dialysis. The consistency of CNC was determined by measuring the weight after completely drying a certain amount of CNC suspension in an oven. The weight of the cellulose raw materials used in each experiment was 5 g, and the CNC yield was calculated based on Eq. 1 as follows:

$$\text{Yield (\%)} = W_1 \text{ (g)} \times W_2 \text{ (\%)} \div 5 \text{ (g)} \quad (1)$$

XRD analysis

The crystallinity index (CrI) and crystallite size (D) of PM-FB and Hw-BKP were characterized using XRD (Bruker D8 Advance A25 Plus, Billerica, MA, USA) operating at 40 kV and 40 mA to evaluate the yield and decomposition of CNCs obtained by sulfuric acid hydrolysis. The PM-FB and Hw-BKP pads were scanned within a 2θ range of 4° to 40°. The crystallinity index (CrI) of the samples was calculated based on Segal's method. Here I_{200} is maximum value in 200 plane, and I_{am} is the minimum value between 110 plane and 200 plane (Segal *et al.* 1959). To derive the crystallinity index, it was calculated using the maximum and minimum intensities,

$$\text{CrI (\%)} = (I_{200} - I_{am})/I_{200} \times 100 \quad (2)$$

$$D \text{ (nm)} = K\lambda / \beta\cos\theta \times 100 \quad (3)$$

where D is the crystallite size of the raw materials (nm), K is the Scherrer constant, λ is the X-ray wavelength, β is full width at half maximum (FWHM), and θ is the Bragg angle (Shahabi-Ghahafarrokhi *et al*. 2015; Zakiyya *et al*. 2020). To determine FWHM, the blank in the background was subtracted, and other manipulations, such as smoothing, were not performed.

Zeta potential of CNCs

The zeta potential of the CNC sample was measured to evaluate its electrostatic characteristics depending on the conditions of the acid hydrolysis process. The CNC suspensions were dispersed at a concentration of 0.1% to 0.2% (w/w) using ultrasonic treatment. Then, 1 mL of the sample was injected into the folded capillary zeta cell using a micro-pipette (P1000, Gilson Inc., Middleton, WI, USA). The zeta potential was measured using a zeta potential analyzer (Nano ZS, Malvern Panalytical, Malvern, UK) at an equilibrium time of 120 s, and the measurements were repeated 3 times.

Fourier transform infrared spectroscopy

Fourier transform infrared (FT-IR) analysis was performed to study the chemical composition of the CNC samples. The CNC film for FT-IR measurement was prepared by a casting method and dried in an oven set to 25 °C. The FT-IR spectra of the CNC films made from PM-FB and Hw-BKP samples were obtained using an FT-IR spectrometer (IS50, Thermo Fisher, Waltham, MA, USA) at the attenuated total reflection mode using 32 scans.

Morphologies of cellulose nanocrystals

The fiber sizes of the CNC particles were measured to evaluate their properties in relation to the cellulose materials and the acid hydrolysis conditions using transmission electron microscopy (TEM) (Talos L120C, ThermoFisher Scientific, Waltham, MA, USA) at an accelerating voltage of 120 kV. A drop of the CNC suspensions diluted to 0.2 g/L was dropped on a 300-mesh silicon-monoxide grid and negative stained with uranyl acetate for 5 min to capture high-contrast images. The fiber length, fiber width, and aspect ratio of 100 individual CNC particles were obtained for each sample based on the TEM image analysis conducted using 3D image software (Axio Vision Rel 4.8, Carl Zeiss, Oberkochen, Germany).

RESULTS AND DISCUSSION

CNC Yield

Figures 2 and 3 show the residual weights and yields of the PM-FB-based CNCs (PM-CNCs) and Hw-BKP-based CNCs (Hw-CNCs) depending on the hydrolysis conditions. Figure 2 was obtained by measuring the total dry weight of the remaining undissolved fibers after sulfuric acid hydrolysis and centrifugation for 10 times. A residue of less than 7% of the total weight was obtained when the PM-FB was hydrolyzed for 45 min at 60 °C and a low concentration of sulfuric acid (55%). However, a residue of 10% to 29% of the total weight was obtained for Hw-BKP even when a high concentration of sulfuric acid (60%) was used. With the increase in the sulfuric acid concentration, hydrolysis time, and temperature, the residual weight gradually decreased. The PM-CNC had a much lower residual weight than Hw-CNC, indicating that more of the fiber material was hydrolyzed by sulfuric acid, resulting in less residual weight. Therefore, this suggests that PM-CNC has a much higher decomposition efficiency than Hw-CNC under the same hydrolysis conditions.

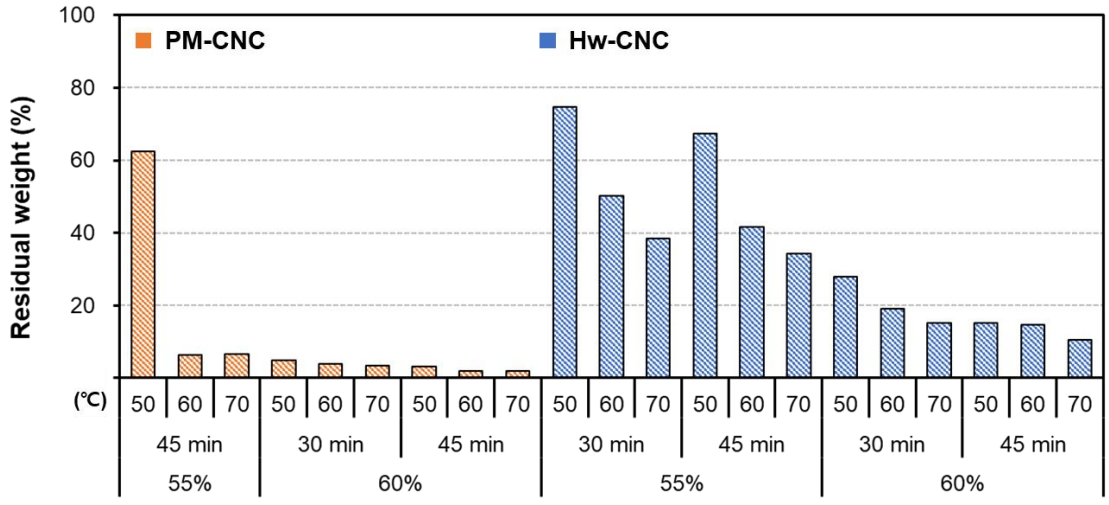

Fig. 2. Residual weights of PM-FB and Hw-BKP

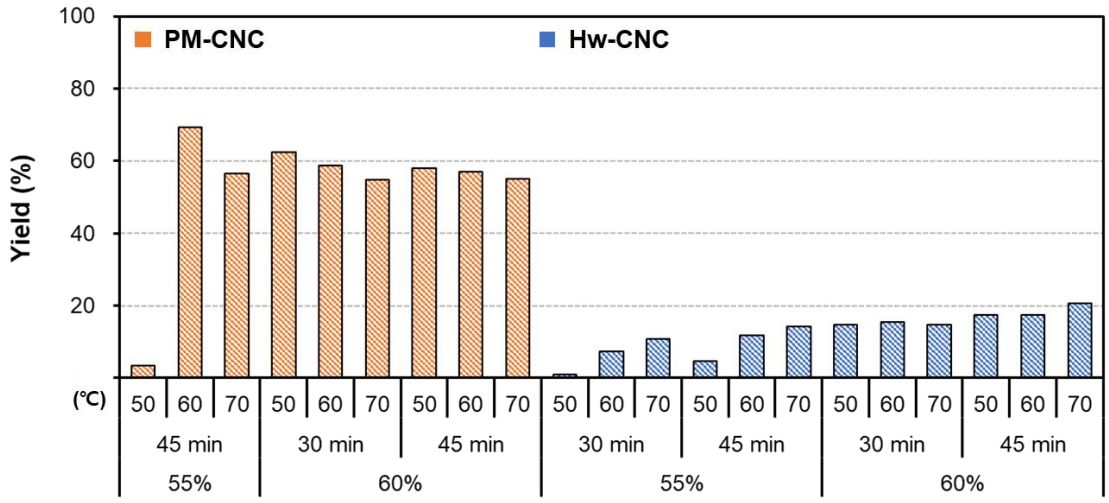

Fig. 3. Yields of PM-CNC and Hw-CNCs

The yields of PM-CNCs and Hw-CNCs were obtained by measuring the amounts and concentrations of CNCs collected after the dialysis (Fig. 3) were 50% or more and 10% to 20%, respectively. This shows that a large difference in the yield can be obtained by changing the raw material. Under stronger hydrolysis conditions, the yield decreased, which can be attributed to the destruction of the β-1,4-glycosidic bonds of cellulose by acid hydrolysis, resulting in the decomposition of cellulose into sugar molecules (Wang *et al*. 2014). This means that the amount of decomposed sugar gradually increased, as a result of excessive hydrolysis and was washed off during the dialysis process. According to a previous study (Kargarzadeh *et al*. 2012), the crystallinity of bast fiber is higher than that of other natural fibers, and hence, they have higher CNC yields. Thus, the CNC yield of mulberry fibers was higher than that of Hw-BKP under relatively mild conditions.

XRD Analysis

The XRD results (Fig. 4 and Table 2) indicated that the crystallinity of PM-FB was 86.8%, which was higher than that of Hw-BKP (77.9%). The XRD spectra of both raw materials showed the main peaks of cellulose I (French 2014; Xing *et al*. 2018). In the XRD spectra of PM-FB, the three peaks observed had Miller indices of plane 1-10, 110, and 200 that were clearer than those of Hw-BKP (Syamani *et al*. 2015; French 2018). The sharp peaks observed only in the PM-FB spectrum may have originated from residual contaminants present in the raw material that is less bleached than Hw-BKP. A similar peak was also observed in a previous study that used unbleached mulberry fiber (Amna *et al.* 2021). The CNCs were manufactured by removing the amorphous region of the cellulose by the acid and leaving only the crystal region, and hence the crystallinity of the raw materials were significantly affected. Therefore a large amount of CNCs may be obtained from PM-FB, which has relatively large crystalline regions. The Hw-BKP exhibited a wide peak width and a low maximum peak height. Moreover, a lower yield was obtained from Hw-BKP compared to PM-FB because Hw-BKP has a relatively high ratio of amorphous regions.

In addition, the crystallite sizes of PM-FB and Hw-BKP were calculated based on their XRD peak widths to be 6.93 and 5.07 nm, respectively. Therefore, PM-FB had a

larger crystallite size. Next, the individual size of the manufactured CNCs was assessed using TEM image analysis (Figs. 7 to 9). The fiber lengths of PM-CNCs and Hw-CNCs were similar, but the fiber width of Hw-CNCs was smaller than that of PM-CNCs. This indicates that PM-FB was sufficiently decomposed under the hydrolysis conditions used in this study to prepare CNCs. In contrast, stronger reaction conditions are needed to manufacture CNCs from Hw-BKP. According to several studies (Boonipitakasakul *et al*. 2019, Sreenivas *et al*. 2020, Sarkar *et al*. 2022), unlike bleached or refined bleached kraft pulp, the content of alpha cellulose in the bast fiber is 61% to 76%. Bleached kraft pulp is processed through multi-stage bleaching using strong alkali treatment and evaporation, in which most of the hemicellulose is eliminated, resulting in an alpha cellulose content of more than 80% (may reach more than 92% depending on the level of purification) (Tripathi *et al*. 2017). According to Xiang *et al*. (2003), the α-cellulose can be completely decomposed under sulfuric acid concentration of more than 65%, which is higher than the hydrolysis conditions used in this study. Therefore, in order to sufficiently hydrolyze Hw-BKP into CNC, a high sulfuric acid concentration and strong reaction conditions (such as time and temperature) that can completely hydrolyze α-cellulose are required, and by controlling the reaction conditions, the yield of Hw-CNC can also be increased. Consequently, the hydrolysis of PM-FB occurs faster than those of Hw-BKP under the same reaction conditions, making it a suitable species for producing high CNC yield.

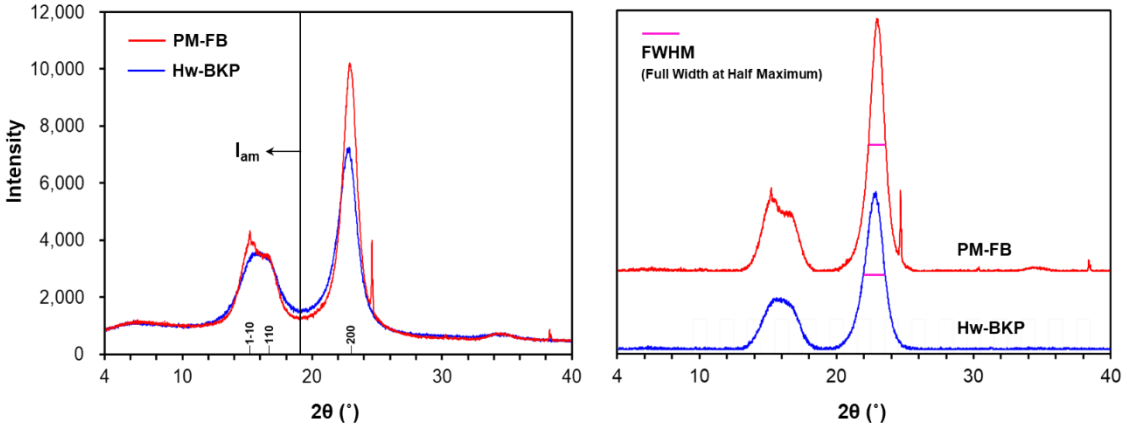

Fig. 4. XRD patterns of PM-FB and Hw-BKP

Table 2. Results of the XRD Analysis of PM-FB and Hw-BKP

Raw Materials	Crystallinity (%)	Crystallite Size (nm)
PM-FB	86.8	6.93
Hw-BKP	77.9	5.07

Electrostatic Properties of CNCs

To evaluate the electrostatic characteristics of the prepared CNCs, their zeta potential was measured by diluting the CNC suspension to 0.2% or less. Basically, the anionic properties of cellulose are stronger after sulfuric acid hydrolysis because a sulfate group is introduced during the process (Fig. 5). These results are confirmed by the FT-IR results (Fig. 6).

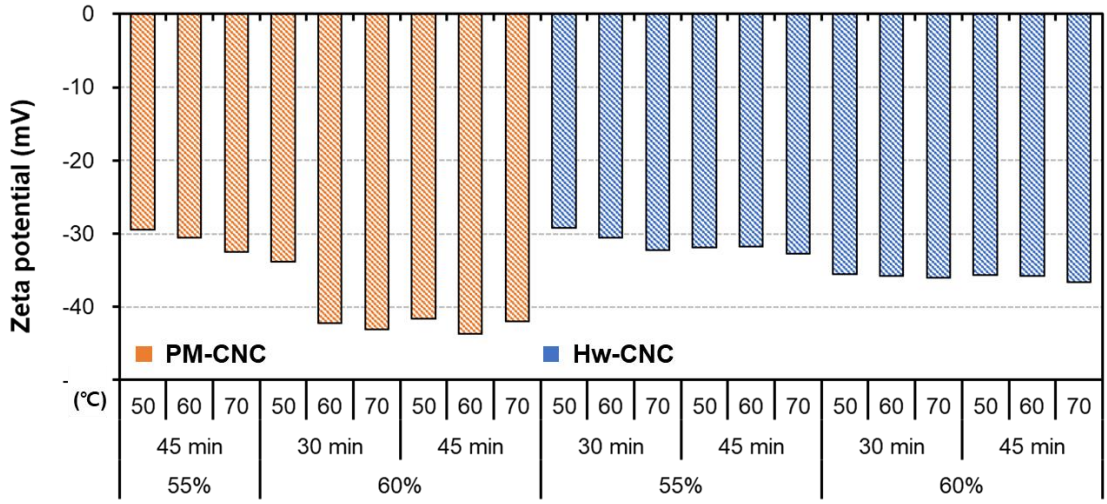

Fig. 5. Zeta potential of PM-CNCs and Hw-CNCs

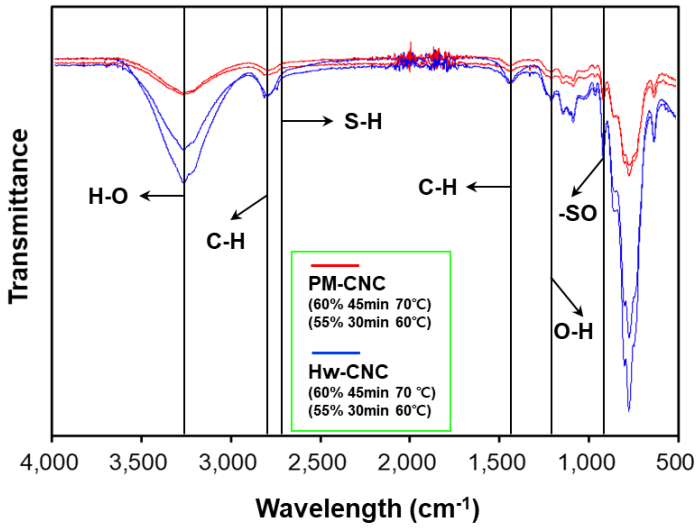

Fig. 6. FT-IR spectra of PM-CNC and Hw-CNCs

A wide peak, which can be attributed to the hydroxyl group of the cellulose, was observed between 3,200 and 3,400 cm^{-1}, and the typical cellulose peaks were observed at 2,900 and 1,430 cm^{-1}. There was no significant difference in the peaks of the cellulose subjected to different hydrolysis levels, and the peaks attributed to the–SH and -SO vibrations were also observed, which confirms the presence of the sulfone group. Under all conditions, weak –SH peaks were observed around 2,700 to 2,800 cm^{-1}, and the peaks of the -SO groups were observed around 790 to 810 cm^{-1}. These results and the reduction of -OH groups confirm the introduction of the sulfone groups (Das *et al*. 2010; Han *et al*. 2013). The zeta potential of cellulose nanofibers (CNFs), which is a nanocellulose produced by mechanical treatment, is −18 to −24 mV (Park *et al*. 2018), and it has a very strong negative charge. Figure 5 shows the zeta potentials of CNCs according to the raw material. Higher absolute values of negative zeta potential was obtained at a high sulfuric acid concentration, and it gradually increased with the increase of the severity of the

reaction conditions. A sulfate group is introduced into CNCs as a result of the esterification of the hydroxyl group on the surface of the cellulose during hydrolysis (Navarro *et al.* 2021). Thus, this hydroxyl group becomes a strong anion, and thus, its zeta potential is reduced. In addition, the increased surface area due to the gradually decreasing CNC fiber size may have also affected the zeta potential. These characteristics increase the colloidal stability of the manufactured CNCs (Vanderfleet *et al.* 2018). Therefore, they can be used in applications that require high dispersibility. The PM-CNCs exhibited higher absolute values of negative zeta potential than Hw-CNCs, which can be attributed to the introduction of sulfonic acid. Moreover, the time for the PM-FB separation into individual CNC particles was shorter than that for Hw-BKP.

Morphology of CNC

Figures 7 to 9 show the TEM images of the individual particles of the prepared CNCs.

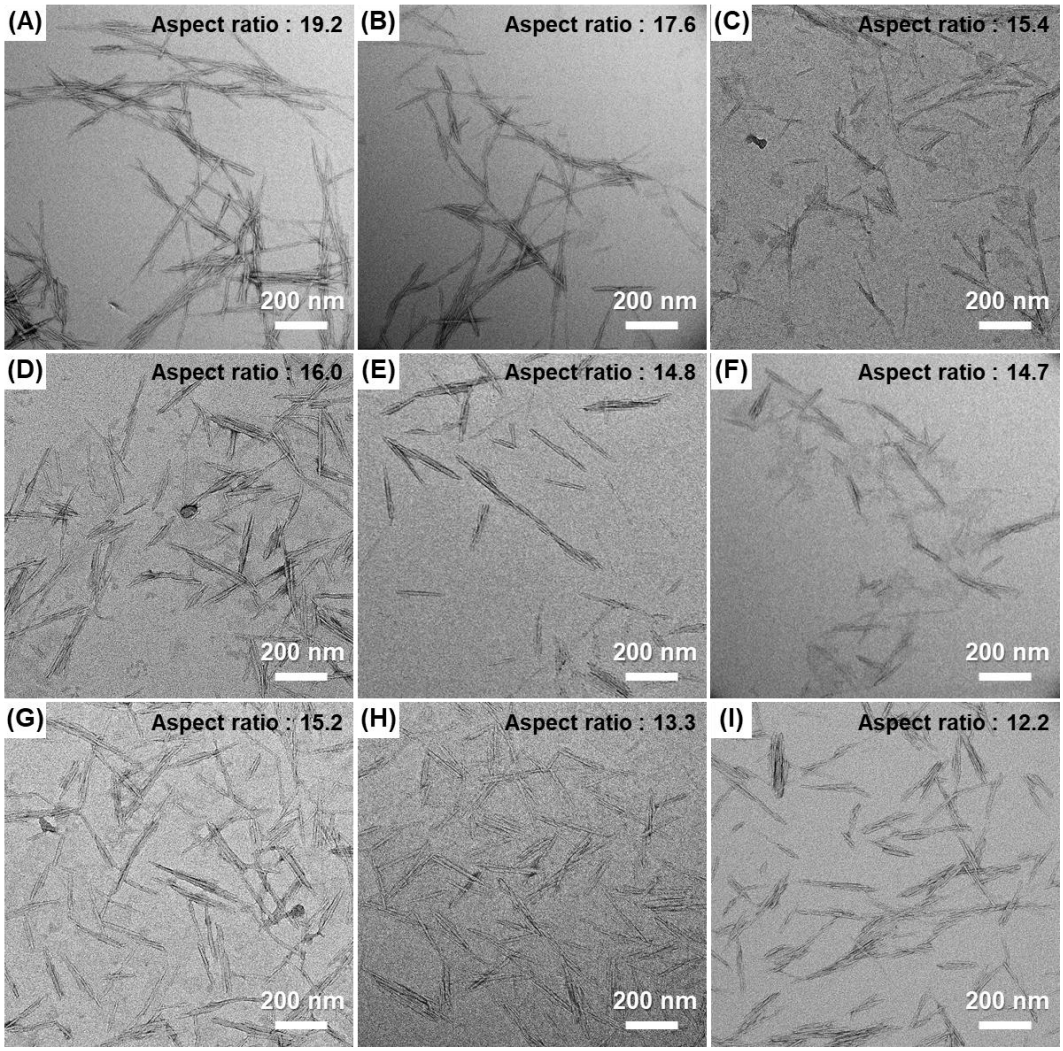

Fig. 7. TEM images and aspect ratios of PM-CNCs under different hydrolysis conditions: (A to C) H_2SO_4 concentration = 55%, and (D to I) H_2SO_4 concentration = 60%

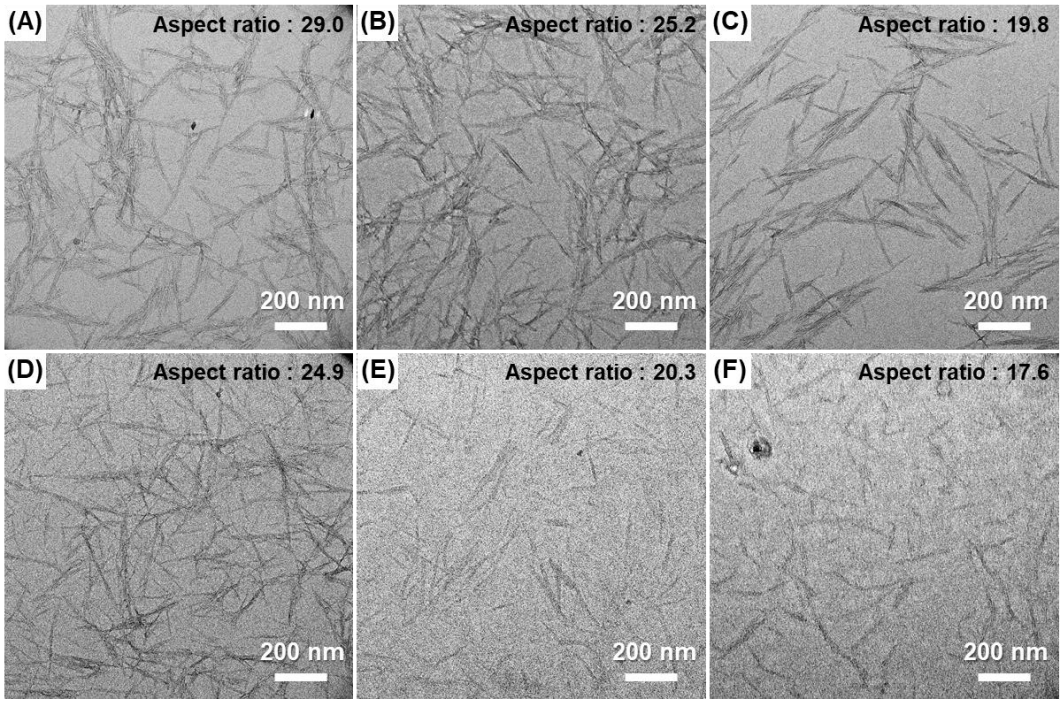

Fig. 8. TEM images and aspect ratios of Hw-CNCs at a H_2SO_4 concentration of 55%

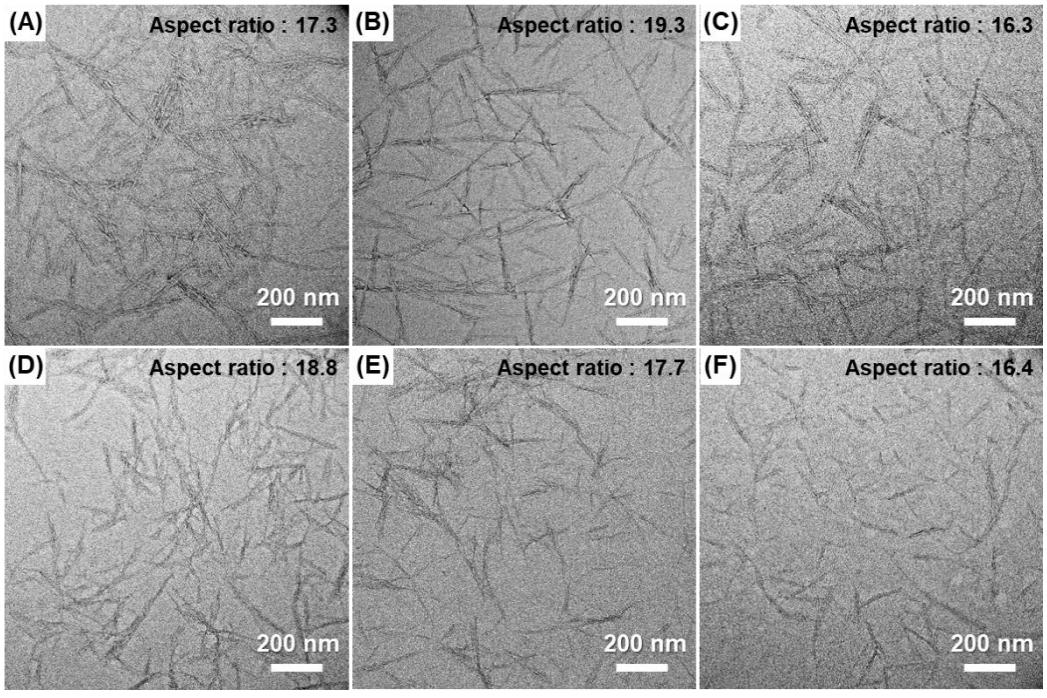

Fig. 9. TEM images and aspect ratios of Hw-CNCs at a H_2SO_4 concentration of 60%

The particle size decreased under stronger sulfuric acid hydrolysis conditions. The CNC shape differed with the type of the raw material used. The fiber width of the Hw-CNCs was smaller than that of the PM-CNCs. The aspect ratio of the PM-CNCs gradually decreased, and the aspect ratio of the fiber width, which is smaller than that of PM-CNCs, was generally increased. The change in the fiber width was not significant, and the aspect ratio decreased with the decrease in the fiber length. Figures 10 and 11 show the average fiber sizes of both raw materials.

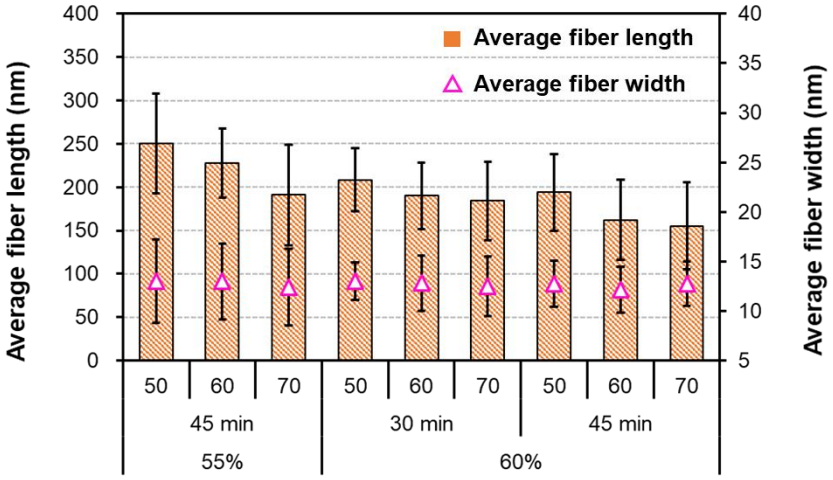

Fig. 10. Average fiber size of PM-CNCs

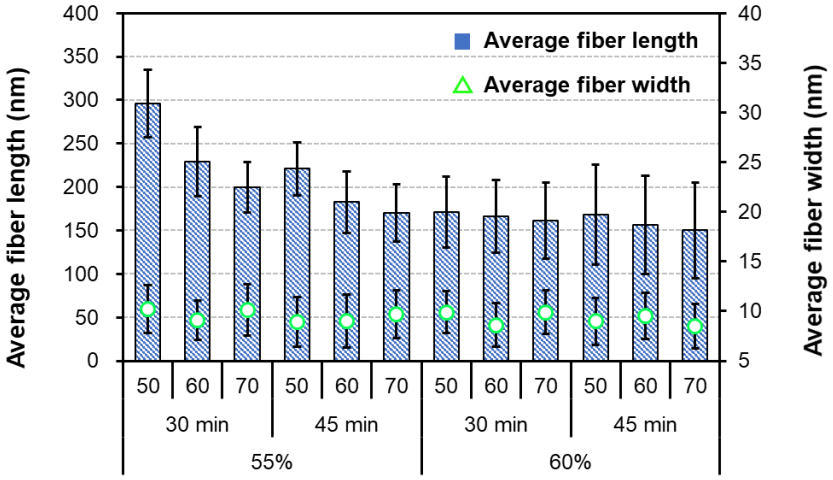

Fig. 11. Average fiber size of Hw-CNCs

Several researchers have reported that smaller fiber sizes are obtained under stronger hydrolysis conditions (Lin *et al*. 2019; Kusmono *et al*. 2020; Yu *et al*. 2021). The fiber size decreased with the increase in the sulfuric acid concentration, reaction temperature, and time, but the fiber width did not show a significant change after the fiber separation into individual CNC particles. The standard deviation value of fiber length does not decrease despite the strong reaction conditions, which can be attributed to the decomposition of some fibers into small CNC particles. This is a similar result to that

obtained for the CNC manufacturing using cotton fiber (Elazzouzi-Hafraoui *et al*. 2008). Under the strongest hydrolysis conditions used in this study, the length and width of PM-CNCs were approximately 155 nm and 12.6 nm, and those of Hw-CNCs were 150 nm and 8.5 nm, respectively. The CNC size obtained in this study is within the range of CNC sizes reported in previous studies and those commercially available (Habibi *et al*. 2010; Moon *et al*. 2011; Delepierre *et al*. 2021). Thus, PM-FB is a suitable non-wood raw material and can generate CNCs at a level similar to that of Hw-BKP but with a higher yield.

CONCLUSIONS

1. The paper mulberry bast fiber (PM-FB) exhibited a higher yield of cellulose nanocrystals (CNCs) than Hw-BKP under mild acid hydrolysis conditions. At the same sulfuric acid concentration, the hydrolysis of PM-FB occurred faster than that of Hw-BKP with a final yield of 50% or more. Because PM-FB has a crystallinity that is approximately 10% higher than that of Hw-BKP, PM-FB is more suitable for CNC manufacturing using acid hydrolysis, where the amorphous region of the raw material is decomposed.
2. Sulfuric acid hydrolysis introduced the anionic sulfonic acid group into the prepared CNCs, which reduced the zeta potential of the materials and the fiber size depending on the hydrolysis conditions. Thus, highly anionic PM-CNCs with high dispersibility were obtained.
3. Different CNC fiber lengths were obtained depending on the level of hydrolysis, but the fiber width was not significantly affected by the hydrolysis conditions. The fiber width of PM-CNCs was larger than that of Hw-CNCs, and hence, Hw-CNCs exhibited a relatively higher aspect ratio than PM-CNCs. Moreover, CNCs with a fiber length and width of 150 to 250 nm and 7 to 13 nm, respectively, were obtained under all conditions.
4. Therefore, a higher CNC yield was obtained using PM-FB under mild reaction conditions than that obtained using Hw-BKP. Both CNCs exhibited similar qualities. Therefore, PM-FB can be used as an eco-friendly raw material with a high CNC yield.

ACKNOWLEDGMENTS

This work was supported by the National Research Foundation of Korea (NRF) grant funded by the Korea Government (MSIT) (No. 2022R1A2C1007565).

REFERENCES CITED

Amna, T., Hassan, M. S., Sheikh, F. A., Seo, H. C., and Kim, H. C. (2021). "Natural mulberry biomass fibers doped with silver as an antimicrobial textile: A new generation fabric," *Textile Research Journal* 91(21-11), 1-7. DOI:10.1177/00405175211013422

Arun, R., Shruthy, R., Preetha, R., and Sreejit, V. (2022). "Biodegradable nano composite reinforced with cellulose nano fiber from coconut industry waste for replacing synthetic plastic food packaging," *Chemosphere* 291, article 132786. DOI:10.1016/j.chemosphere.2021.132786

Boonipitaksakul, W., Chitbanyong, K., Puangsin, B., Pisutpiched, S., and Khantayanuwong, S. (2019). "Natural fibers derived from coi (*Streblus asper* Lour.) and their behavior in pulping and as paper," *Bioresources* 14(3), 6411-6420. DOI:10.15376/biores.14.3.6411-6420

Cong, R., and Dong, W. (2007). "Structure and property of mulberry fiber," *Modern Applied Science* 1(4), 14-17. DOI:10.5539/mas.v1n4p14

Das, K., Ray, D., Bandyopadhyay, N. R., and Sengupta, S. (2010). "Study of the properties of microcrystalline cellulose particles from different renewable resources by XRD, FTIR, nanoindentation, TGA and SEM," *Journal of Polymers and the Environment* 18, 355-363. DOI:10.1007/s10924-010-0167-2

Delepierre, G., Vanderfleet, O. M., Niinivaara, E., Zakani, B., and Cranston, E. D. (2021). "Benchmarking cellulose nanocrystals part II: new industrially produced materials," *Langmuir* 37(28), 8393-8409. DOI:10.1021/acs.langmuir.1c00550

de Souza Fonseca, A., Panthapulakkal, S., Konar, S. K., Sain, M., Bufalinof, L., Raabe, J., de Andrade Miranda, I. P., Martins, M. A., and Tonoli, G. H. D. (2019). "Improving cellulose nanofibrillation of non-wood fiber using alkaline and bleaching pre-treatments," *Industrial Crops and Products* 131, 203-212. DOI:10.1016/j.indcrop.2019.01.046

Domingues, R. M. A., Gomes, M. E., and Reis, R. L. (2014). "The potential of cellulose nanocrystal in tissue engineering strategies," *Biomacromolecules* 15(7), 2327-2346. DOI:10.1021/bm500524s

Dong, S., Bortner, M. J., and Roman, M. (2016). "Analysis of the sulfuric acid hydrolysis of wood pulp for cellulose nanocrystal production: A central composite design study," *Industrial Crops and Products* 93, 76-87. DOI:10.1016/j.indcrop.2016.01.048

Elazzouzi-Hafraoui, S., Nishiyama, Y., Putaux, J. L., Heux, L., Dubreuil, F., and Rochas, C. (2008). "The shape and size distribution of crystalline nanoparticles prepared by acid hydrolysis of native cellulose," *Biomacromolecules* 9(1), 57-65. DOI:10.1021/bm700769p

French, A. D. (2014). "Idealized powder diffraction patterns for cellulose polymorphs," *Cellulose* 21, 885-896. DOI:10.1007/s10570-013-0030-4

French A. D. (2018). "Cellulose," in: *Encyclopedia of Biophysics*, Roberts, G., and Watts, A. (eds.), Springer, Berlin, Germany, pp. 1-9. DOI:10.1007/978-3-642-35943-9_82-1

George, J. and Sabapathi, S. N. (2015). "Cellulose nanocrystals: synthesis, functional properties, and applications," *Nanotechnology*, Science and Applications 8, 45-54. DOI:10.2147-NSA.S64386

Grishkewich, N., Mohammed, S., Tang, J., and Tam, K. C. (2017). "Recent advances in the application of cellulose nanocrystals," *Current Opinion in Colloid & Interface Science* 29, 32-45. DOI: 10.1016/j.cocis.2017.01.005

Guo, C., and Guo, H. (2022). "Progress in the degradability of biodegradable film materials for packaging," *Membranes* 12(5), article 500. DOI: 10.3390/membranes12050500

Habibi, Y., Lucia, L. A., and Rojas, O. J. (2010). "Cellulose nanocrystals: Chemistry, self-assembly, and applications," *Chemical Reviews* 110, 3479-3500. DOI:10.1021/cr900339w

Han, J., Zhou, C., Wu, Y., Liu, F., and Wu, Q. (2013). "Self-assembling behavior of cellulose nanoparticles during freeze-drying: effect of suspension concentration, particle size, crystal structure, and surface charge," *Biomacromolecules* 14(5), 1529-1540. DOI:10.1021/bm4001734

Hu, D., and Ma, W. (2020). "Nanocellulose as a sustainable building block to construct eco-friendly thermally conductive composites," *Industrial & Engineering Chemistry Research* 59, 19465-19484. DOI:10.1021/acs.iecr.0c04319

Jones, D., Ormondroyd, G. O., Curling, S. F., Popescu, C. M., and Popescu, M. C. (2017). "Chemical compositions of natural fibers," in: *Advanced High Strength Natural Fibre Composites in Construction*, Fan, M., and Fu, F. (eds.), Woodhead Publishing, Sawston, UK, pp. 23-58. DOI:10.1016/B978-0-08-100411-1.00002-9

Kandhola, G., Djioleu, A., Rajan, K., Labbe, N., Sakon, J., Carrier, D. J., and Kim, J. W. (2020). "Maximizing production of cellulose nanocrystals and nanofibers from pre-extracted loblolly pine kraft pulp: A response surface approach," *Bioresources and Bioprocessing* 7(1), 1-16. DOI:10.1186/s40643-020-00302-0

Kargarzadeh, H., Ahmad, I., Abdullah, I., Dufresne, A., Zainudin, S. Y., and Sheltami, R. M. (2012). "Effects of hydrolysis conditions on the morphology, crystallinity, and thermal stability of cellulose nanocrystals extracted from kenaf bast fibers," *Cellulose* 19, 855-866. DOI:10.1007/s10570-012-9684-6

Kargupta, W., Seifert, R., Martinez, M., Olson, J., Tanner, J., and Batchelor, W. (2021). "Sustainable production process of mechanically prepared nanocellulose from hardwood and softwood: A comparative investigation of refining energy consumption at laboratory and pilot scale," *Industrial Crops and Products* 171, article 113868. DOI:10.1016/j.indcrop.2021.113868

Kusmono, Listyanda, R. F., Wildan, M. W., and Ilman, M. N. (2020). "Preparation and characterization of cellulose nanocrystal extracted from ramie fibers by sulfuric acid hydrolysis," *Heliyon* 6(11), article e05486. DOI:10.1016/j.heliyon.2020.e05486

Li, T., Chen, C., Brozena, A. H., Zhu, J. Y., Xu, L., Driemeier, C., Dai, J., Rojas, O. J., Isogai, A., Wagberg, L., and Hu, L. (2021). "Developing fibrillated cellulose as a sustainable technological material," *Nature* 590(7844), 47-56. DOI: 10.1038/s41586-020-03167-7.

Lin, K. H., Enomae, T., and Chang, F. C. (2019). "Cellulose nanocrystal isolation from hardwood pulp using various hydrolysis conditions," *Molecules* 24(20), article 3724. DOI:10.3390/molecules24203724

Navarro, S. L., Nakayama, K., Idstrom, A., Evenas, L., Strom, A., and Nypelo, T. (2021). "The effect of sulfate half-ester groups on cellulose nanocrystal periodate oxidation," *Cellulose* 28, 9633-9644. DOI:10.1007/s10570-021-04115-y

Moshood, T. D., Nawanir, G., Mahmud, F., Mohamad, F., Ahmad, M. H., and Ghani, A. A. (2022). "Biodegradable plastic applications towards sustainability: A recent innovations in the green products," *Cleaner Engineering and Technology* 6, article 100404. DOI:10.1016/j.clet.2022.100404

Moon, R. J., Ashlie, M., John, N., John, S., and Jeff, Y. (2011). "Cellulose nanomaterials review: structure, properties and nanocomposites," *Chemical Society Reviews* 40(7), 3941-3994. DOI:10.1039/C0CS00108B

Park, J. Y., Park, C. W., Han, S. Y., Kwon, G. J., Kim, N. H., and Lee, S. H. (2019). "Effects of pH on nanofibrillation of TEMPO-oxidized paper mulberry bast fibers," *Polymers* 11(3), 414. DOI: 10.3390/polym11030414

Park, T. U., Lee, J. Y., Jo, H. M., and Kim, K. M. (2018). "Utilization of cellulose micro/nanofibrils as paper additive for the manufacturing of security paper," *BioResources* 13(4), 7780-7791. DOI: 10.15376/biores.13.4.7780-7791

Rajinipriya, M., Nagalakshmaiah, M., Robert, M., and Elkoun, S. (2018). "Importance of agricultural and industrial waste in the field of nanocellulose and recent industrial developments of wood based nanocellulose: A review," *ACS Sustainable Chemistry Engineering* 6, 2807-2828. DOI: 10.1021/acssuschemeng.7b03437

Samir, A., Ashour, F. H., Hakim, A. A. A., and Bassyouni, M. (2022). "Recent advances in biodegradable polymers for sustainable applications," *NPJ Materials Degradation* 6(1), 1-28. DOI: 10.1038/s1529-022-00277-7

Sarkar, S., Dilruba, F. A., Rahman, M., Hossen, M., Dayan, A. R., Khatton, A., Sarker, J., and Uddin, M. (2022). "Isolation of microcrystalline alpha-cellulose from jute: A suitable and economical viable resource," GSC *Biological and Pharmaceutical Sciences* 18(03), 219-225. DOI:10.30574/gscbps.2022.18.3.0121

Seddiqi, H., Oliaei, E., Honarkar, H., Jin, J., Geonzon, L. C., Bacabac, R. G., and Nulend, J. K. (2021). "Cellulose and its derivatives: Towards biomedical applications," *Cellulose* 28, 1893-1931. DOI:10.1007/s10570-020-03674-w

Segal, L., Creely, J. J., Martin, J. A. E., and Conrad, C. M. (1959). "An empirical method for estimating the degree of crystallinity of native cellulose using the X-ray diffractometer," *Textile Research Journal* 29(10), 786-794.

Shahabi-Ghahafarrokhi, I., Khodaiyan, F., Mousavi, M,. and Yousefi, H. (2015). "Preparation and characterization of nanocellulose from beer industrial residues using acid hydrolysis/ultrasound," *Fibers and Polymers* 16, 529-536. DOI:10.1007/s12221-015-0529-4

Sreenivas, H. T., Krishnamurthy, N., and Arpitha, G. R. (2020). "A comprehensive review on light weight kenaf fiber for automobiles," *International Journal of Lightweight Materials and Manufacture* 3(4), 328-337. DOI:10.1016/j.ijlmm.2020.05.003

Syamani, F. A., Subyakto, S., Suryani, S. A. (2015). "Changes in oil palm frond fiber morphology, cellulose crystallinity and chemical functional groups during cellulose extraction phases," *Chemistry and Materials Research* 7(3), 105-114.

Tang, Y., Yang, H., and Vignolini, S. (2022). "Recent progress in production methods for cellulose nanocrystals: Leading to more sustainable processes," *Advanced Sustainable Systems* 6(3), article 2100100. DOI:10.1002/adsu.202100100

Thakur, S., Chaudhary, J., Sharma, B., Verma, A., Tamulevicius, S., and Thakur, V. (2018). "Sustainability of bioplastics: Opportunities and challenges," *Current Opinion in Green and Sustainable Chemistry* 13, 68-75. DOI:10.1016/j.cogse.2018.04.013

Tripathi, G., Sinha, A. R., and Tomar, M. (2017). "Effect of different types of wood pulp on hydrolysis reaction time and degree of polymerization of microcrystalline cellulose powder," *World Journal of Pharmaceutical Research* 6(9), 733-742. DOI:10.20959/wjpr20179-9252

Vanderfleet, O. M., Osorio, D., and Cranston, E. D. (2018). "Optimization of cellulose nanocrystal length and surface charge density through phosphoric acid hydrolysis," *Philosophical Transactions of the Royal Society: A Mathematical, Physical and Engineering Sciences* 376, 2017001. DOI:10.1098/rsta.2017.0041

Wang, Q., Zhao, X., and Zhu, J. Y. (2014). "Kinetics of strong acid hydrolysis of a bleached kraft pulp for producing cellulose nanocrystals (CNCs)," *Industrial & Engineering Chemistry Research* 53(27), 11007-11014. DOI:10.1021/ie501672m

Xiang, Q., Lee, Y. Y., Pettersson, P. O., and Torget, R. W. (2003). "Heterogeneous aspects of acid hydrolysis of a-cellulose," in*: Biotechnology for fuels and Chemicals*, Davison, B. H., Lee, J. W., Finkelstein, M., and McMillan, J. D. (eds.), Springer Science Business Media, Berlin, Germany, pp.505-514.

Xina, L., Gu, J., Zhang, W., Tu, D., and Hu, C. (2018). "Cellulose I and II nanocrystals produced by sulfuric acid hydrolysis of Tetra Pak cellulose I," *Carbohydrate Polymer* 195, 184-192. DOI:10.1016/j.carbpol.2018.03.042

Yu, X., Jiang, Y., Wu, Q., Wei, Z, Lin, X., and Chen, Y. (2021). "Preparation and characterization of cellulose nanocrystal extraction from *Pennisetum hydridum* fertilized by municipal sewage sludge via sulfuric acid hydrolysis," *Frontiers in Energy Research* 9, article 774783. DOI:10.3389/fenrg.2021.774783

Yu, Y., Wang, Q., and Wang, P. (2019). "Bioprocessing of bast fibers," in: *Advances in Textile Biotechnology*, Cavaco-Paulo, A., Nierstrasz, V. A., and Wang, Q. (eds.), Woodhead Publishing, Sawston, UK, pp. 1-19. DOI:10.1016/B978-0-08-102632-8.00001-3

Zakiyya, U., Uyunin, Masruri, M., Ningsih, Z., and Srihardyastutie, A. (2020). "Sonication-assisted pine cone flower cellulose hydrolysis using formic acid," *IOP Conference Series: Materials Science and Engineering* 833, article 012001. DOI:10.1088/1757-899X/833/1/012001

Zinge, C, and Kandasubramanian, B. (2020). "Nanocellulose based biodegradable polymers," *European Polymer Journal* 133, article 109758. DOI:10.1016/j.eurpolymj.2020.109758

Article submitted: February 14, 2023; Peer review completed: March 25, 2023; Revised version received and accepted: April 10, 2023; Published: April 24, 2023.
DOI: 10.15376/biores.18.2.4055-4070